World Academy of Science, Engineering and Technology
International Journal of Materials and Metallurgical Engineering
Vol:8, No:12, 2014

The Interaction between Hydrogen and Surface Stress in Stainless Steel

O. Takakuwa, Y. Mano, H. Soyama

***Abstract*—**This paper reveals the interaction between hydrogen and surface stress in austenitic stainless steel by X-ray diffraction stress measurement and thermal desorption analysis before and after being charged with hydrogen. The surface residual stress was varied by surface finishing using several disc polishing agents. The obtained results show that the residual stress near surface had a significant effect on hydrogen absorption behavior, that is, tensile residual stress promoted the hydrogen absorption and compressive one did opposite. Also, hydrogen induced equi-biaxial stress and this stress has a linear correlation with hydrogen content.

***Keywords*—**Hydrogen embrittlement, Residual stress, Surface finishing, Stainless steel.

I. Introduction

THE objective of the present study is to reveal the interaction between hydrogen and surface stress in austenitic stainless steel.

Hydrogen easily invades and diffuses into metals, causing a decrease in tensile ductility, making the metal brittle and accelerating fatigue crack growth [1]. This is known as hydrogen embrittlement [2]. Hydrogen diffuses in accordance with its concentration and stress gradient [3]. Also hydrogen has a tendency to concentrate around a crack tip and/or inclusion etc. where hydrostatic stress is high. So, residual stress field may affect hydrogen absorption and diffusion. Recently, a technique has been developed to suppress this, employing surface modification, which introduces high compressive residual stress near surface [4]. By numerical analysis, the compressive residual stress mitigates stress concentration around a crack tip due to crack closure effect; as a result, hydrogen concentration around the crack tip can be prevented by the compressive residual stress [5]. Therefore the residual stress has a potential to significantly affect hydrogen absorption behavior and it should be revealed, because the residual stress is easily introduced by heat treatment and mechanical surface finishing.

In recent study, hydrogen varies mechanical properties near surface of metallic materials. It has been shown, using an indentation test, that hydrogen hardens the surface of austenitic stainless steel [6-8] and increases yield stress from 300 MPa to 620 MPa [9]. Hydrogen becomes trapped in the lattice, dislocations, grain boundaries or defects. When hydrogen is trapped at lattice sites, it leads to changes in both the micro- and macro-strains [10]. The micro-strain refers to the strain between adjacent grains and the random strain within grains. Hydrogen trapped at lattice sites can increase the strain in the lattice. The macro-strain is a more homogeneous quantity and is on a larger scale involving many grains, i.e., hydrostatic stress. In this case, the hydrostatic stress is affected by the presence of hydrogen. Therefore, there is an interaction between hydrogen and surface stress field.

In this study, the residual stress near surface of austenitic stainless steel was varied by several surface finishing treatments and then the variations in surface stress for each surface due to hydrogen charging was evaluated using an X-ray diffraction method. Also, hydrogen content was evaluated by a thermal desorption analysis using gas chromatography.

O. Takakuwa is an assistant professor at Tohoku University, Sendai, 9808579 Japan (corresponding author to provide phone: +81-(0)22-795-6899; fax: +81-(0)22-795-3758; e-mail: o_takakuwa@mm.mech.tohoku.ac.jp).

Y. Mano is a student of Graduate School of Engineering at Tohoku University, Sendai, 9808579 Japan

H. Soyama is a professor at Tohoku University, Sendai, 9808579 Japan

II. Experimental Apparatus and Procedures

The material under test was Japanese Industrial Standards JIS SUS316L austenitic stainless steel which has a higher resistance to hydrogen embrittlement than both ferritic and martensitic steel. SUS316L has been applied for hydrogen station and components for hydrogen supply. The samples used in this study were square, 25 mm on each side, and 4 mm thick. The yield stress defined as a 0.2 % offset stress and the tensile strength were 304 MPa and 576 MPa, respectively. The chemical composition was shown in Table I.

A. Hydrogen Charging

Hydrogen absorption was carried out by employing a cathodic charging method as shown in Fig. 1. The solution used for this was 0.5 mol/l sulfuric acid at a temperature of 50 degree Celsius, and charging was done by controlling the current at a current density of 1.0 mA/mm^2. The cathodic and anodic electrodes were the sample and a platinum wire, respectively. Hydrogen was generated at the cathode, i.e., on the sample. Thus, the sample surface was exposed to hydrogen during the cathodic hydrogen charging. For each sample, the area exposed to hydrogen was 20 mm in diameter. X-ray diffraction measurements were done on samples that had been charged with hydrogen for various times ranging from 0 to 48 hours.

TABLE I
The Chemical Composition of SUS316L

Element	C	Si	Mn	P	S	Ni	Cr	Mo
Content (wt. %)	0.014	0.63	0.97	0.030	0.004	12.03	17.45	2.05

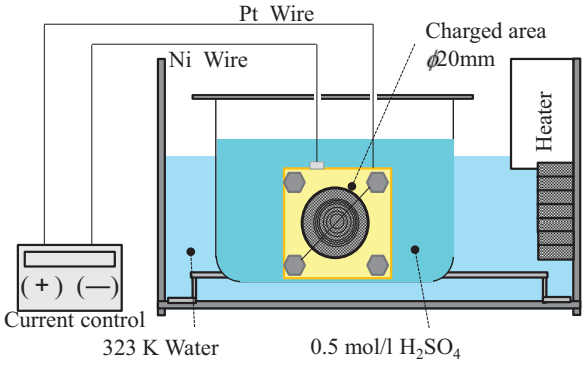

Fig. 1 Apparatus for the cathodic hydrogen charging

B. Surface Finishing

In order to generate various residual stresses near surface, surface finishing was done on the surface using four types of commercially available disc grinder which had a diameter of 100 mm as shown in Fig. 2. These discs were named as A/W36 (AW); manufactured by NIPPON RESIBON COOPRATION, Scotch-Bright (SB); manufactured by Sumitomo 3M, N-Strip (NS); manufactured by Sumitomo 3M and GP-DX (GD); manufactured by TRASCO. The rotating speed was set to 11,000 rpm The direction of residual stress caused by the disc grinder was defined rotating and scanning direction of the disc as *x* and *y*, respectively, due to anisotropic residual stress. After the preparation, residual stress measurements were carried out in accordance with following conditions.

(a) A/W36 (AW) (b) Scotch-Bright (SB)

(c) N-Strip (NS) (d) GP-DX (GD)

Fig. 2 Polishing agent for surface finishing

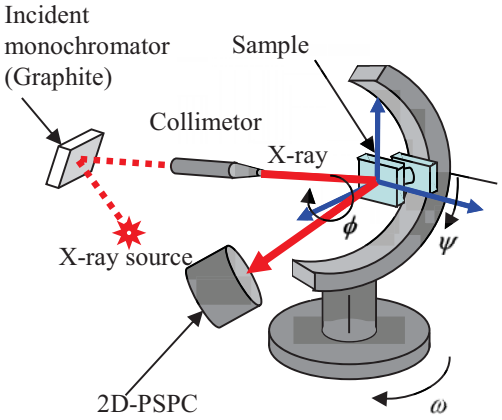

Fig. 3 Geometry of the diffractometer

TABLE II
THE ANGLES OF ϕ AND ψ

ψ	ϕ
0	0
30	0, 45, 90, 135, 180, 225, 270, 315
60	0, 45, 90, 135, 180, 225, 270, 315

C. X-ray Diffraction Stress Measurements

The surface stress, i.e., residual stress, was evaluated by a two-dimensional X-ray diffraction method employing a two dimensional position sensitive proportional counter (2D-PSPC). The stress measurements were conducted using Cr-Kα X-rays from a tube operated at 35 kV and 40 mA through a 0.8 mm diameter collimator and with an incident monochromator. The tested sample was placed in the diffractometer. The geometry is shown in Fig. 3. The diffraction ring from the sample was detected by 2D-PSPC with the angles denoted as ϕ and ψ angles. The stress tensors were calculated by a relationship between the angles and the diffraction ring distortion. The angles of ϕ and ψ were chosen as described in Table II by reference to the past report [11]. The detecting time was 120 s.

D. Thermal Desorption Analysis

In order to evaluate hydrogen content for each sample, the thermal desorption analysis was done using a gas chromatography as shown in Fig. 4. The tested sample was placed in a tube furnace which had an inner diameter of 44 mm, length of 500 mm and volumetric capacity of 1 L. The temperature was increased with the rate of temperature rising of 200 degree Celsius/h and kept at 800 degree Celsius for 1 h. In the furnace tube, Ar gas was flowed at 1mL/s. The gas flowing out of furnace tube was trapped in a 50mL syringe. Hydrogen has been included in the top 10mL of gas trapped in the syringe. 5 mL of this gas was analyzed by using a gas chromatograph with thermal conductivity detector TCD. Ar gas of 99.9998% was used as a carrier gas, career pressure was 600 kPa, column temperature and TCD temperature was 130 and 180 degree Celsius, respectively, and TCD bridge current was 60 mA. On this chromatographic system, peak of hydrogen appears from the retention time of 1.5 min to 3 min. The integrated intensity from 1.5 min to 3min was defined as the relative amount of

hydrogen Q. Hydrogen content, C_H, had been corrected by a relationship between Q and pure hydrogen gas content. In this experiment, samples were charged with hydrogen for 24 h.

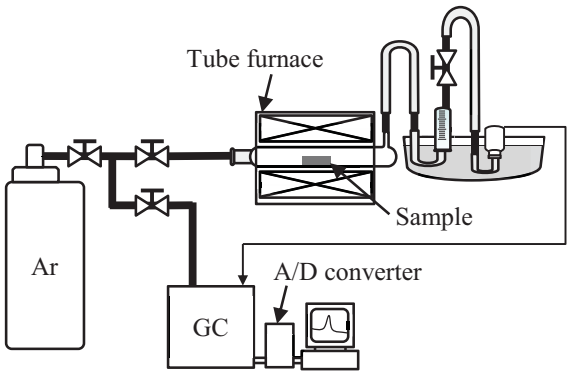

Fig. 4 Apparatus for the thermal desorption analysis

III. Results

Fig. 5 shows the variation of residual stress, σ_R, as a function of hydrogen charging time, t_c, at x (Rotating direction) and y (Scanning direction) directions for each sample. The positive value shows tensile residual stress and the negative does opposite. In Fig. 5, before being charged with hydrogen, high tensile residual stress was introduced in AW and compressive residual stress was introduced in SB, NS and GD. All samples had an anisotropic stress due to the rotating and scanning direction. The residual stress induced by the surface finishing might depend on temperature when the disc contacts the surface. The contact temperature higher than transition temperature of metal provides tensile residual stress. In AW, large tensile residual stress (σ_{Rx}, σ_{Ry}) = (742, 320) MPa was introduced in the rotating direction. On the other hand, in NS, large compressive residual stress (σ_{Rx}, σ_{Ry}) = (-253, -507) MPa was introduced. The surface roughness was (Ra_x, Ra_y) = (0.26, 1.31) μm for AW, (0.20, 0.44) μm for SB, (0.22, 0.53) μm for NS and (0.24, 0.56) μm for GD. The surface roughness should have very few effects on the hydrogen charging, since the hydrogen charging was controlled by the current density in this study. After being charged with hydrogen, the residual stress in both x and y directions in all samples shifted to compression and its variation became saturated at t_c = 24 h. That is, the equi-biaxial compressive stress was generated by hydrogen charging. For instance, in AW and NS, the residual stress varied from (σ_{Rx}, σ_{Ry}) = (742, 320) MPa to (205, -105) and from (σ_{Rx}, σ_{Ry}) = (-253, -507) MPa to (-425, -670), respectively. So as to make the variation easier to understand, Fig. 6 shows the stress variation in the rotating direction between before and after being charged with hydrogen, $\Delta\sigma_{Rx}$, as a function of the charging time, t_c, for each sample. As shown in Fig. 6, at t_c = 24 h, $\Delta\sigma_{Rx}$ was 531 MPa for AW and 172 MPa for NS. Thus, the amount of stress variation differs by the type of the surface finishing, i.e., residual stress before being charged with hydrogen. Hydrogen trapped in lattice intends to expand volume of the lattice and a reactive stress, i.e., the equi-biaxial compressive stress, should be generated. From the result in the variation of the stress, the residual stress near surface affects the hydrogen absorption behavior. That is, the tensile and compressive residual stress may accelerate and prevent the hydrogen absorption, respectively, into the surface as referred in the past report [5]. Also, the reactive stress against hydrogen in the lattice may have a relationship with hydrogen content.

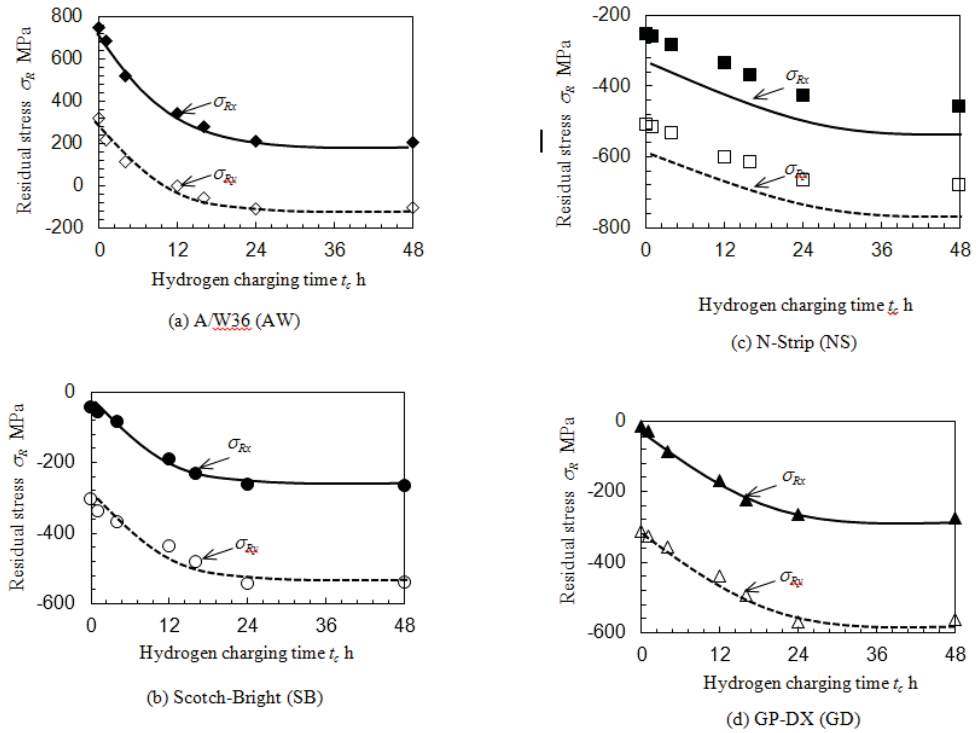

Fig. 5 Variation of the residual stress due to hydrogen charging

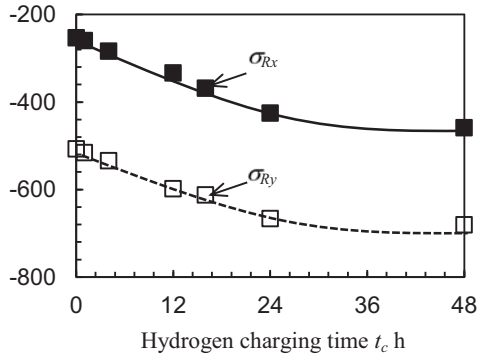

(c) N-Strip (NS)

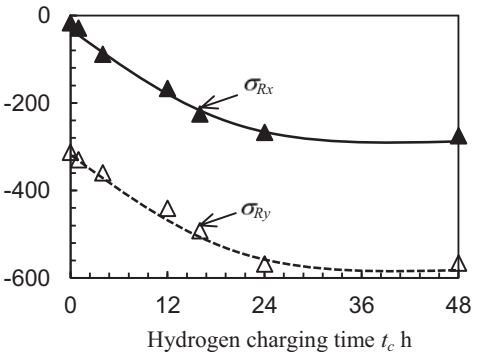

(d) GP-DX (GD)

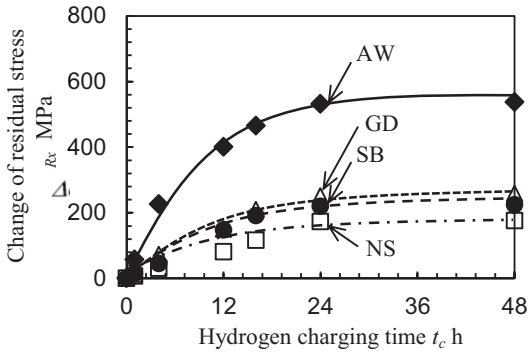

Fig. 6 Change of the residual stress due to hydrogen charging versus hydrogen charging time for each surface finishing

In order to verify the hydrogen content, Fig. 7 shows gas chromatograph at the charging time of 24 h for all samples obtained from the thermal desorption analysis. The peaks around retention time of 2 min represent peaks due to hydrogen. The hydrogen content was calculated by the integral intensity of each peak. From the result, the hydrogen content, C_H, was 4.33 wt. ppm for AW, 1.72 wt. ppm for SB, 1.61 wt. ppm for NS, 2.28 wt. ppm for GD. There is a significant difference in the hydrogen content between AW and NS. The difference is probably due to the difference in the residual stress near surface.

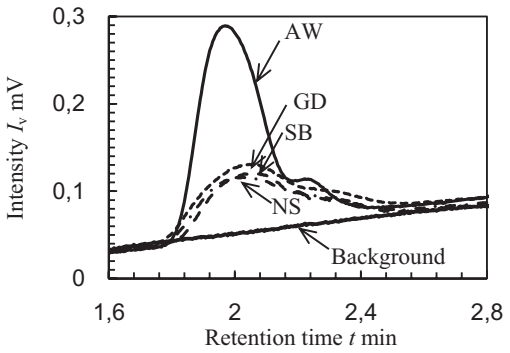

Fig. 7 Variation of hydrogen absorption due to surface finishing

Fig. 8 shows hydrogen content at the charging time of 24 h, C_H, as a function of residual stress before being charged with hydrogen in the rotating direction as a representative, σ_{Rx}. As shown in Fig. 8, the hydrogen content was linearly increased along with increase in the residual stress. It is quite likely that the tensile residual stress expands atomic spacing near surface and the compressive residual stress does opposite. It leads to promotion or suppression of the hydrogen absorption into the surface. This result enhances a hypothesis of which the compressive can prevent hydrogen embrittlement [4], [5], [7].

Fig. 9 shows hydrogen content at the charging time of 24 h, C_H, as a function of the variation of the residual stress in rotating direction before and after being charged with hydrogen, i.e., hydrogen-induced stress, σ_{HIS}. As shown in Fig. 9, there is a linear correlation between hydrogen content and hydrogen-induced stress. Therefore, the variation of the residual stress is attributed to hydrogen trapped in the lattice site, e.g., octahedral site. The austenitic stainless steel has a very high capacity to which hydrogen is absorbed in the lattice site. As a result, the surface stress was varied by which large amount of hydrogen was absorbed.

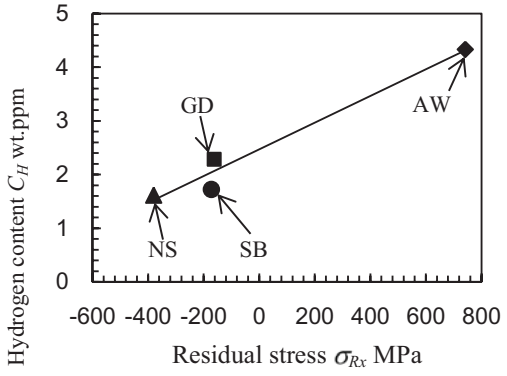

Fig. 8 Increase in hydrogen content along with increase in residual stress

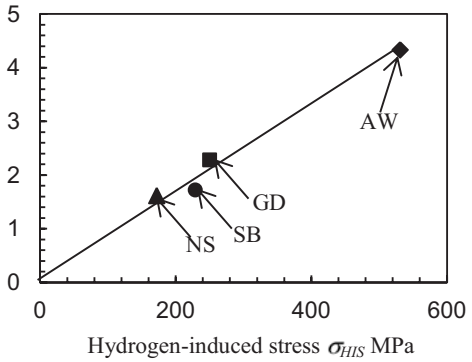

Fig. 9 Relationship between hydrogen content and hydrogen-induced stress

There is an interaction between the surface residual stress and hydrogen content. The residual stress varies the hydrogen absorption behavior. The tensile residual stress promotes it and the compressive stress prevents it. When hydrogen is absorbed in the lattice site, e.g., octahedral site, this provides a reactive compressive stress, i.e., hydrogen-induced stress, and magnitude of the hydrogen-induced stress depends on the hydrogen content. Therefore, this interaction will lead to a method to evaluate local hydrogen content around a crack tip and/or heat affected zone of welding where severe hydrogen effect is generated. In addition, type of the mechanical surface finishing needs to be optimized from the viewpoint of the surface residual stress so as to manufacture hydrogen structure components.

IV. Conclusions

In the present paper, in order to reveal the interaction between surface stress and hydrogen, the residual stress was introduced by surface finishing using four types of disc polishing agents and the surface was charged with hydrogen, and the stress before and after being charged with hydrogen was evaluated by X-ray diffraction stress measurement employing a 2D method. Also, hydrogen content was evaluated by thermal desorption analysis using a gas chromatography. The obtained results are summarized as follows:

1. The residual stress near surface affects hydrogen absorption behavior. The tensile residual stress promotes the hydrogen absorption into the surface and the compressive residual stress prevents it.
2. Hydrogen trapped in lattice site induces a reactive stress, i.e., hydrogen-induced stress, and magnitude of the hydrogen-induced stress is dependent on the hydrogen content. There is a close relationship between the hydrogen content and the hydrogen-induced stress.

Acknowledgment

This work was partly supported by JSPS KAKENHI Grant number 24360040 and 25820001, and Hitachi Metals Materials Science Foundation.

References

[1] Y. Murakami, T. Kanezaki, Y. Mine and S. Matsuoka, "Hydrogen Embrittlement Mechanism in Fatigue of Austenitic Stainless Steels," *Metall. Mater. Trans. A*, vol. 39, no. 6, pp. 1327–1339, 2008.
[2] W.H. Johnson, "On some remarkable changes produced in iron and steel by the action of hydrogen and acids," *Proc. Royal Society of London*, vol. 23, pp. 168–179, 1874.
[3] A.T. Yokobori, Jr., T. Nemoto, K. Satoh and T. Yamada, "Numerical analysis on hydrogen diffusion and concentration in solid with emission around the crack tip," *Eng. Fract. Mech.*, vol. 55, no. 1, pp. 47–60, 2002.
[4] O. Takakuwa and H. Soyama, "Suppression of hydrogen-assisted fatigue crack growth in austenitic stainless steel by cavitation peening," *Int. J. Hydrogen Energy*, vol. 37, no. 6, pp. 5268–5276, 2012.
[5] O. Takakuwa, M. Nishikawa and H. Soyama, "Numerical simulation of the effects of residual stress on the concentration of hydrogen around a crack tip," *Surf. Coat. Technol.*, vol. 206, no. 11–12, pp. 2892–2898, 2012.
[6] A. Barnoush and H. Vehoff, "Recent developments in the study of hydrogen embrittlement: Hydrogen effect on dislocation nucleation," *Acta Mater.*, vol. 58, no. 16, pp. 5274–5285, 2010.
[7] O. Takakuwa and H. Soyama, "Using an indentation test to evaluate the effect of cavitation peening on the invasion of the surface of austenitic stainless steel by hydrogen," *Surf. Coat. Technol.*, vol. 206, no. 18, pp. 3747–3750, 2012.
[8] O. Takakuwa, Y. Mano and H. Soyama, "Effect of indentation load on Vickers hardness of austenitic stainless steel after hydrogen charging," *Proc. ASME Pressure Vessel & Piping Conf.*, pp. 28280–1–6, 2014.
[9] O. Takakuwa, Y. Mano and H. Soyama, "Increase in the local yield stress near surface of austenitic stainless steel due to invasion by hydrogen," *Int. J. Hydrogen Energy*, vol. 39, no. 11, pp. 6095–6103, 2014.
[10] O. Takakuwa, Y. Mano and H. Soyama, "(24) Effect of hydrogen on the micro- and macro-strain near the surface of austenitic stainless steel," *Adv. Mater. Research*, vol. 936, pp. 1298–1302, 2014.
[11] O. Takakuwa and H. Soyama, "Optimizing the conditions for residual stress measurement using a two-dimensional XRD method with specimen oscillation," *Adv. Mater. Phys. Chem.*, vol. 3, no. 1A, pp. 8–18, 2013.